ChemComm

COMMUNICATION

View Article Online
View Journal | View Issue

Cite this: *Chem. Commun.*, 2018, **54**, 4325

Received 12th February 2018,
Accepted 29th March 2018

DOI: 10.1039/c8cc01264d

rsc.li/chemcomm

Singular wavelength dependence on the sensitization of lanthanides by graphene quantum dots†

Meredith McDowell,[a] Andrew Metzger,[a] Chong Wang,[bc] Jiming Bao,[c] James M. Tour *[ade] and Angel A. Martí *[adf]

In this manuscript, we study the sensitization of Tb^{3+} ions by the excited state of GQD. We found that Tb^{3+} cations can bind to GQDs and display photoluminescence. Excitation dependent experiments show that the Tb^{3+} emission is stronger at shorter excitation wavelengths, which is likely due to pseudo-isolated small aromatic moieties produced during the synthesis of the GQDs.

Graphene quantum dots (GQDs) are nanoparticles which are structurally similar to small graphene nanoflakes. Similar to inorganic quantum dots, GQDs exhibit bright fluorescence upon light irradiation where their emission wavelength shows an hypsochromic shift with decreasing particle size. Our group has previously reported a synthesis of GQDs from coal, making this material water soluble and affordable for mass production.[1] These GQDs do not show a shift in emission with change in excitation, which is common in many carbon dot preparations.[2,3] The top down synthesis leads to some heterogeneity within each sample and therefore wide absorption and emission bands are obtained. Sorting of GQDs by size results in fractions with different emission wavelengths that are characteristic of their size.[22] These properties makes GQDs suitable candidates for antennae in solar cells, bioimaging and sensing applications.[4]

Rare earth elements are valuable for their distinct photophysical properties. Spin forbidden f–f* excitations have low extinction coefficients and long phosphorescence lifetimes.[5] Because the f orbitals are shielded and they interact very little with ligands, their spectral bands are very sharp (10 nm wide).[5] These traits lead to their use in solid state lasers[6] and as imaging agents.[7] Terbium(III) (Tb^{3+}), frequently doped into the YAG crystal, has an $^5D_4$ excited state which decays down to the ^7F ground state with strongest emissions at *ca.* 489 nm, 544 nm, 584 nm, and 621 nm.[5,8,9] Tb^{3+} salts have low extinction coefficients and require ligands with accessible triplet states to sensitize their emission,[8] although singlet sensitization has been claimed in certain cases.[8,10]

In this manuscript, we will explore the sensitization of the rare earth Tb^{3+} cation by GQDs. There have been reports of indium oxide quantum dots sensitizing europium(III);[11] however, to our knowledge this is the first report of GQDs being used to sensitize rare earth cations. Blue-GQDs (bGQDs) were obtained from liberating graphitic nanodomains naturally present in coal using chemical oxidation, and they can contain a variety of functional groups on their surface such as carboxylic acids, sulfates, nitrates, and hydroxyl groups, which can potentially bind lanthanide cations. We expect GQDs to have a dual function: (1) act as polydentate ligands binding the lanthanide cations and (2) transfer energy to the lanthanide excited states resulting in long-lived lanthanide photoluminescence. The excitation and emission photoluminescence spectra of bGQDs are presented in Fig. 1a. As is typical for bGQDs, the emission spectrum shows a broad peak with a maximum of ~435 nm. Addition of different concentrations of $TbCl_3$ to bGQDs led to the appearance of new peaks in the photoluminescence spectrum that are consistent with the $^5D \rightarrow {}^7F$ emission bands of Tb^{3+} at *ca.* 489, 544, 584 and 621 nm (Fig. 1b). These conjugates of bGQDs and Tb^{3+} were called Tb@bGQDs. The initial excitation wavelength was chosen at 330 nm, which is far from the weak absorption peak of Tb^{3+} in the ultraviolet (Fig. S1, ESI†). Still, while the Tb^{3+} cation shows a shoulder from 230–300 nm (Fig. S1, ESI†) it only shows low intensity emission unless coordinated to a photosensitizer ligand. Plotting the area corresponding to Tb^{3+} photoluminescence as a function of Tb^{3+} concentration shows that maximum photoluminescence is obtained at ~3 μM Tb^{3+}, (although concentrations from 1 to 10 μM still yield quite acceptable photoluminescence) with a decrease in

[a] *Department of Chemistry, Rice University, Houston TX 77005, USA. E-mail: tour@rice.edu, amarti@rice.edu*
[b] *School of Material Science and Engineering, Yunnan University, Kunming, China*
[c] *Department of Electrical and Computer Engineering, University of Houston, Houston TX 77004, USA*
[d] *Department of Material Science & Nanoengineering, Rice University, Houston TX 77005, USA*
[e] *Smalley-Curl Institute and Nanocarbon Center, Rice University, Houston TX 77005, USA*
[f] *Department of Bioengineering, Rice University, Houston TX 77005, USA*

† Electronic supplementary information (ESI) available: Experimental methods and supporting spectra and experiments. See DOI: 10.1039/c8cc01264d

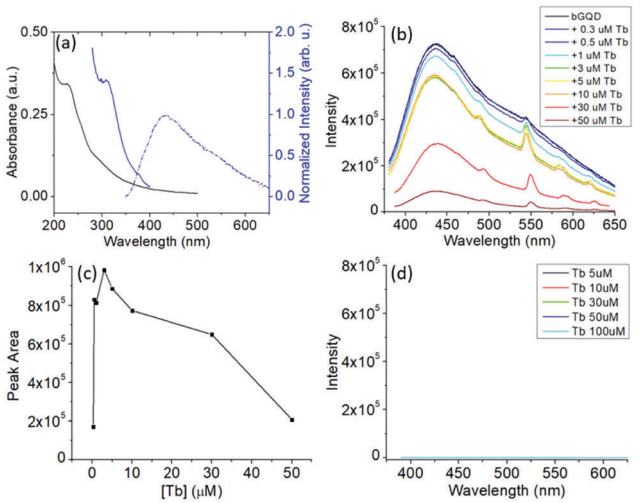

Fig. 1 (a) Absorption (black), excitation (solid blue) and emission (dashed blue) spectra of bGQDs (5 μg mL^{-1}) in water excited at 330 nm. (b) Emission spectra of $TbCl_3$ titration into aqueous solution of bGQDs. (c) Plot of emission area of the 545 nm peak from the $TbCl_3$ titration in (b). (d) Photoluminescence of $TbCl_3$ at varying concentrations in water excited at 330 nm with the same scale as (b).

photoluminescence with increasing Tb^{3+} concentration (Fig. 1c). This decrease could be due to self-quenching upon binding of multiple Tb^{3+} to a single GQD. A similar behavior has been observed for Tb^{3+} incorporated in poly(vinyl pyrrolidone) and have been attributed to microscopic Tb^{3+} aggregates where efficient intermolecular energy transfer occurs leading to quenching.[12] Control experiments with the same concentrations of Tb^{3+} in water as in Fig. 1b led to no noticeable photoluminescence (Fig. 1d), which confirms that bGQDs are photosensitizing the Tb^{3+} ^5D excited state. To probe whether this photosensitization is due to an intra or intermolecular energy transfer process, we added ethylenediaminetetraacetic acid (EDTA) to Tb@bGQDs (Fig. S2, ESI†). EDTA is a strong chelating agent and is expected to bind more strongly to Tb^{3+} than bGQDs, stripping the lanthanide cation from the surface of the bGQDs. Addition of EDTA to Tb@bGQDs causes an immediate disappearance of the Tb^{3+} photoluminescence, and the complete recovery of the bGQDs photoluminescence (Fig. S2, ESI†), which proves that binding of Tb^{3+} to bGQDs is a requirement for photosensitization to take place, and thus the sensitization reaction is intramolecular. Moreover, we observed that the photoluminescence of the bGQDs decreases with increasing Tb^{3+} concentration (Fig. 1b). This is likely related to quenching of bGQDs by the heavy paramagnetic Tb^{3+} cation by promoting intersystem crossing to the triplet state. A similar behavior is observed when bGQDs are titrated with Gd^{3+} (Fig. S3, ESI†), which is a paramagnetic rare earth with a similar size to Tb^{3+}, but that does not have low-lying energy levels (below 32 000 cm^{-1}) that can be sensitized by bGQDs.[13] Sensitization of Tb^{3+} commonly occurs from the population of a triplet state of the photosensitizer, following by energy transfer to the $^5D_4$ excited state level of Tb^{3+} (at 20 400 cm^{-1}). Nonetheless, some reports have stated that, in certain cases, the singlet excited state of the sensitizer has a big role in the population of Tb^{3+} excited states.[14] Steady-state photoluminescence experiments in air and with samples purged with nitrogen were performed. Samples of Tb@bGQDs purged with nitrogen present almost twice the photoluminescence from Tb^{3+} than samples in air (Fig. S4, ESI†). The photosensitization dependence with oxygen is consistent with triplet states in bGQDs close in energy with the ^5D energy levels in of the Tb^{3+} allowing energy back transfer. The triplet state repopulation makes it susceptible to quenching by molecular oxygen, causing a decrease in the Tb^{3+} emission.

The excited state lifetime of bGQDs is presented in Table 1. The photoluminescence lifetime of bGQDs purged with nitrogen at 435 nm is 3.3 ns, which is consistent with the decay lifetime from a short-lived singlet-state. Experiments in a frozen matrix of ethanol/methanol (77 K) did not show new peaks or shifts, nor the appearance of a longer lifetime component. Nonetheless, the phosphorescence of triplet excited states is generally difficult to see even at 77 K, since the long-lived lifetime competes with non-radiative deactivation pathways. Furthermore, these triplet state could be dark states and invisible to fluorescence techniques. To evaluate the existence of triplet states in bGQDs, NIR photoluminescence experiments were preformed to test for the presence of singlet oxygen. Triplet molecular oxygen can be converted into singlet molecular oxygen by energy transfer from a triplet photosensitizer. The phosphorescence spectrum for singlet oxygen was clearly observed at 1273 nm for bGQD

Table 1 Photophysical parameters for bGQD and Tb@GQD

Sample	ϕTb[a]	ϕGQD[a]	τ_{435nm}[b]	τ_{545nm}[c]
bGQDs	—	0.09 ± 0.01	0.54 ± 0.01 ns (20%)	—
			2.26 ± 0.03 ns (56%)	—
			8.3 ± 0.2 ns (24%)	—
			$\langle\tau\rangle$ = 3.3 ns	—
Tb@bGQDs	0.009 ± 0.001	0.024 ± 0.003	0.213 ± 0.003 ns (42%)	175 ± 7 μs (20%)
			1.37 ± 0.02 ns (39%)	640 ± 10 μs (80%)
			7.6 ± 0.1 ns (19%)	—
			$\langle\tau\rangle$ = 2.0 ns	$\langle\tau\rangle$ = 530 μs

[a] λ_{ex}: 250 nm, λ_{em}: 375–700 nm. [b] λ_{ex}: 371 nm. [c] λ_{ex}: 330 nm.

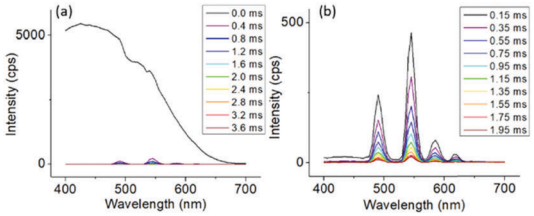

Fig. 2 TRES of Tb@bGQDs excited at 330 nm showing spectra recorded (a) 0–3.6 ms and (b) 0.15–1.95 ms after excitation.

and the known $^1O_2$ photosensitizer phenalenone, which is consistent with the generation of long-lived triplet states by the photoexcitation of bGQDs (Fig. S5a and b, ESI†). Notice that no emission at 1273 nm is observed in the sample purged with N_2 (Fig. S5c, ESI†). While this observation is consistent with triplet states in bGQD, this does not rule out that singlet states have some contribution to the photosensitization of Tb@bGQDs.

Time-resolved emission spectroscopy was used to obtain information about the different components in Tb@bGQDs. As stated before, bGQDs have a multicomponent short-lived photoluminescence with average lifetime of 3.3 ns (λ_{em} = 435 nm) in aqueous solution and of 2.0 ns in Tb@bGQDs, while Tb^{3+} (λ_{em} = 545 nm) in Tb@bGQDs has a two-component long-lived photoluminescence with an average lifetime of 533 μs. These differences in lifetimes are evident when the time resolved emission spectra (TRES) are obtained for Tb@bGQDs (Fig. 2). When the TRES spectra are obtained after 0.15 ms, all the background fluorescence from the bGQDs disappears, displaying only the features of Tb^{3+} phosphorescence.

The effect of excitation wavelength on the photoluminescence of Tb@bGQDs was also analyzed. A 3D plot showing the dependence of the photoluminescence as a function of the excitation wavelength for bGQDs, Tb@bGQDs and Tb^{3+} in water are shown in Fig. 3. All the spectra in the three panels were obtained and plotted with exactly the same parameters. It is immediately noticeable that the photoluminescence of bGQDs is quenched by the binding of Tb^{3+}. In addition, no appreciable photoluminescence is observed for the free Tb^{3+} cation under the tested experimental

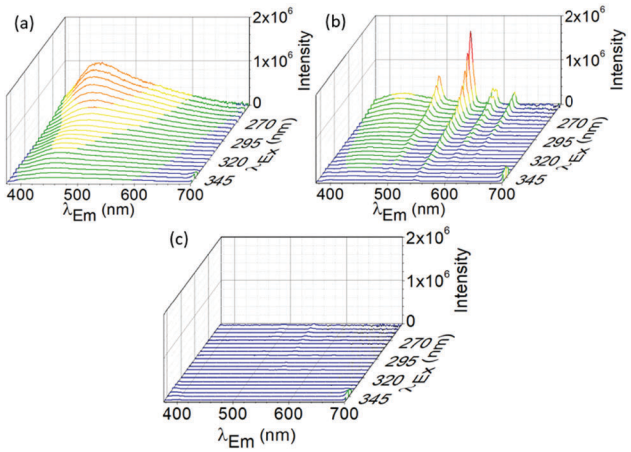

Fig. 3 3D emission spectra of (a) bGQD (10 μg mL^{-1}) (b) Tb@bGQD (10 μg mL^{-1} and 6 μM) and (c) $TbCl_3$ (6 μM).

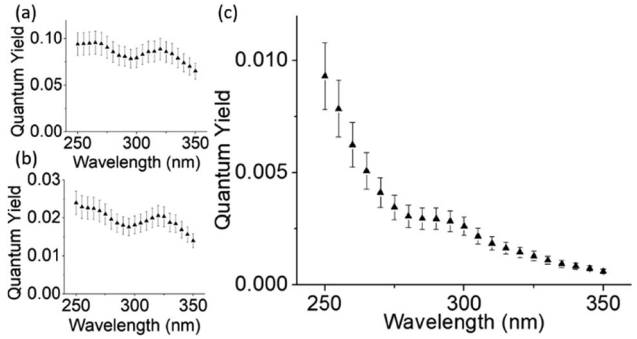

Fig. 4 Quantum yield at varying excitation wavelengths (a) bGQD, (b) the bGQD peak from Tb@bGQD, and (c) the Tb^{3+} peaks from Tb@bGQD.

conditions. The most remarkable observation is that the emission from Tb^{3+} in the Tb@GQDs sample increases at shorter excitation wavelengths. Since we use corrected spectra, knowing the emission quantum yields with excitation at 250 nm from Table 1, and correcting for the inefficiency of the lamp at different wavelengths, it is possible to calculate the quantum yields as a function of excitation (Fig. 4). The quantum yield seems to be independent of wavelength for bGQDs (Fig. 4a). This is consistent with the Kasha–Vavilov rule: the photoluminescence quantum yield is independent of excitation wavelength.[15] For Tb@GQDs, two emissions can be studied: the residual photoluminescence from bGQDs and the photoluminescence from Tb^{3+}. The quantum yield from the photoluminescence of bGQDs is lower due to the presence of Tb^{3+}, however it only shows slight variations with wavelength (Fig. 4b), and in general it just looks similar to Fig. 4a but with lower quantum yield. On the other hand, the photoluminescence from Tb^{3+} shows a strong wavelength dependence, showing a marked increase at shorter excitation wavelengths (Fig. 4c). This increase is approximately an order of magnitude larger with excitation at 250 nm when compared with the photoluminescence exciting at 350 nm.

Although the reason for this deviation from the Kasha–Vavilov rule is unclear, we propose that it is due to small aromatic fragments on the periphery of the GQD core (Fig. 5) that could be directly participating in the photosensitization of Tb^{3+}. The

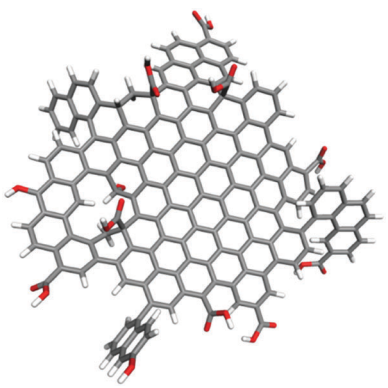

Fig. 5 Schematic showing sp^2 carbon core with oxidative defects. Small organic molecule-like moieties on the periphery could partake in binding and sensitizing Tb^{3+}.

GQDs studied here were prepared from a top-down approach by separating graphitic nanodomains present in coal using a chemically oxidative process; however, workup ensures that small aromatic moieties are not physiosorbed carboxylate carbonaceous fragments.[16] These GQDs are soluble in water due to a variety of functional groups (*e.g.* hydroxyl, carboxyl, *etc.*) induced by the oxidation in H_2SO_4/HNO_3 used to liberate the GQDs from coal. Carefully controlling the reaction conditions and filtration through 1 and 3 kD membranes (see Methods in ESI†) lead to control in the size of the nanodomains, which then influence the color of the GQDs.[1] It is expected that chemical oxidation creates defects that isolate small aromatic moieties that can then act as individual triplet sensitizers (see Fig. 5). For example, small aromatic molecules such as 1,2,4,5-benzenetetracarboxylic acid,[17] 1,4-phenylenediacetate,[18] *p*-aminobenzoic acid,[19] 2,3-dihydroxynaphthalene,[20] and 2,6-naphthalenedicarboxylic acid[21] have been shown to photosensitize Tb^{3+} photoluminescence. Thus, it is possible that GQDs derived from coal are composed by a graphene core surrounded by a corona of small aromatic molecules (covalently attached to the GQD) capable of photosensitizing the photoluminescence of lanthanide ions such as Tb^{3+}. The presence of small aromatic groups derived from a large graphitic core has been observed previously in the synthesis of water-soluble ultra-short single-walled carbon nanotubes by strong oxidation process.[16] These molecules are spectroscopically invisible either because they are weakly fluorescent, or because their fluorescence is quenched by the bGQD core by π stacking or some other mechanism. The absorption of these simple aromatic molecules increases in the blue part of the spectrum, which is consistent with the increased quantum yield of Tb^{3+} at shorter wavelengths. Binding of Tb^{3+} would promote intersystem crossing into the triplet state of many of these moieties, which are capable of photosensitizing Tb^{3+}.

To further explore the sensitization of Tb^{3+} by GQDs we used red-shifted GQDs (rGQDs), which have an emission maximum of 520 nm (Fig. S6, ESI†), and present a bathochromic shift of 85 nm from bGQDs. Interestingly, rGQDs also show sensitization of Tb^{3+} (Fig. S6b, ESI†) with maximum sensitization at 3 μM (5 μg mL^{-1} rGQDs concentration) (Fig. S6c, ESI†). Tb@rGQDs shows a short-lived rGQDs lifetime corresponding to rGQD as well as long lived lifetimes of 553 μs at 545 nm (Table S1, ESI†). Similar to Tb@bGQDs, the quantum yield of emission for Tb^{3+} seems to increase at shorter wavelengths, which can be easily observed in the 3D spectrum in Fig. S7 (ESI†). Given that rGQD are red shifted, which would result in triplet states of lower energy than bGQD, this supports the argument that sensitization comes from the corona of aromatic microdomains in both bGQDs and rGQDs.

In conclusion, binding of Tb^{3+} occurs by the coordination of Tb^{3+} to functional groups on the surface of GQDs such as carboxylic acids, and leads to a unique emission pattern consisting of the superimposition of the sharp long-lived Tb^{3+} bands over the broad short-lived GQD emission. The two emission signals can be separated in the TRES using time-resolve spectroscopy due to their very different lifetimes. Quantum yield experiments as a function of wavelength indicate that bGQDs apparently does not follow the Kasha–Vavilov rule, with higher quantum yields at blue excitation wavelengths. We believe the higher quantum yields at more energetic wavelengths come from small semi-discrete organic moieties attached to the main graphitic domain of GQDs, which are a byproduct of their top-down synthesis. To the best of our knowledge, this represents the first example of rare earth photosensitization using GQDs. The unique properties of this nanoarchitectures can have important implications in the design of photoluminescent sensors, labeling, and as inimitable anti-counterfeit dyes and inks.

James M. Tour thanks the Air Force Office of Scientific Research for support (FA9550-14-1-0111). Jiming Bao acknowledges support from the Robert A. Welch Foundation (E-1728).

Conflicts of interest

Rice University has licensed intellectual property on coal-derived GQDs to a company in which James M. Tour is a stockholder, though not an officer, director or employee. All potential conflicts are managed by regular disclosure to the Rice University Office of Sponsor Programs and Research Compliance.

Notes and references

1 R. Ye, C. Xiang, J. Lin, Z. Peng, K. Huang, Z. Yan, N. P. Cook, E. L. Samuel, C.-C. Hwang, G. Ruan, G. Ceriotti, A.-R. O. Raji, A. A. Martí and J. M. Tour, *Nat. Commun.*, 2013, **4**, 3943.
2 Y.-P. Sun, B. Zhou, Y. Lin, W. Wang, K. A. S. Fernando, P. Pathak, M. J. Meziani, B. A. Harruff, X. Wang, H. Wang, P. G. Luo, H. Yang, E. Kose, B. Chen, L. M. Veca and S.-Y. Xie, *J. Am. Chem. Soc.*, 2006, **128**, 7756–7757.
3 H. Chen, Y. Xie, A. M. Kirillov, L. Liu, M. Yu, W. Liu and Y. Tang, *Chem. Commun.*, 2015, **51**, 5036–5039.
4 X. Li, M. Rui, J. Song, Z. Shen and H. Zeng, *Adv. Funct. Mater.*, 2015, **25**, 4929–4947.
5 K. A. Gschneidner, J.-C. G. Bünzli and V. K. Pecharsky, *Handbook on the physics and chemistry of rare earths, optical spectroscopy*, Elsevier, 2007, vol. 37.
6 M. J. Weber, *Lanthanide and Actinide Chemistry and Spectroscopy*, Lawrence Livermore Laboratories, Livermore, CA, 1980, pp. 275–311.
7 A. J. Amoroso, S. J. A. Pope, A. Nonat, J.-M. Barbe, F. Denat, Y. Chang, T.-J. Kim, K. M. Kim, J. M. Moloney, T. J. Norman, D. Parker, L. Royle, J. A. G. Williams, A. Payn, T. Schild, L. Scola and A. Sinanna, *Chem. Soc. Rev.*, 2015, **44**, 4723–4742.
8 J.-C. G. Bunzli and S. V. Eliseeva, in *Lanthanide Luminescence: Photophysical, Analytical and Biological Aspects*, ed. P. Hanninen, H. Harma and T. Ala-Kleme, Springer-Verlag, Berlin, 2010, pp. 1–45.
9 P. Atkins, T. Overton, J. Rourke, M. Weller and F. Armstrong, in *Inorganic Chemistry*, ed. P. Atkins, T. Overton, J. Rourke, M. Weller and F. Armstrong, Oxford University Press, Oxford, 5th edn, 2010.
10 M. J. Kleinerman, *Chem. Phys.*, 1969, **51**, 2370–2381.
11 J. Vela, B. S. Prall, P. Rastogi, D. J. Werder, J. L. Casson, D. J. Williams, V. I. Klimov and J. A. Hollingsworth, *J. Phys. Chem. C*, 2008, **112**, 20246–20250.
12 L. Quan, T. Li and J. Wu, *J. Phys. Chem. B*, 2001, **105**, 12293–12296.
13 G. A. Hebbink, S. I. Klink, L. Grave, P. G. B. Oude Alink and F. C. J. M. van Veggel, *Chem. Phys. Chem.*, 2002, **3**, 1014–1018.
14 J. R. G. Thorne, J. M. Rey, R. G. Denning, S. E. Watkins, M. Etchells, M. Green and V. Christou, *J. Phys. Chem. A*, 2002, **106**, 4014–4021.
15 A. D. McNaught and A. Wilkinson, in *IUPAC Compendium of Chemical Terminology*, ed. M. Nic, J. Jirat, B. Kosata and A. Jenkins, Blackwell Scientific Publications, Oxford, 2nd edn, 1997.
16 B. K. Price, J. R. Lomeda and J. M. Tour, *Chem. Mater.*, 2009, **21**, 3917–3923.
17 S. Li, X. Zhang, Z. Hou, Z. Cheng, P. Ma and J. Lin, *Nanoscale*, 2012, **4**, 5619–5626.
18 D. K. Singha, S. Bhattacharya, P. Majee, S. K. Mondal, M. Kumar and P. Mahata, *J. Mater. Chem. A*, 2014, **2**, 20908–20915.
19 D. Ghosh and M. N. Luwang, *RSC Adv.*, 2015, **5**, 10468–10478.
20 K. P. Divya and R. G. Weiss, *J. Phys. Chem. Lett.*, 2015, **6**, 893–897.
21 S. Maji and K. S. Viswanathan, *J. Lumin.*, 2008, **128**, 1255–1261.
22 R. Ye, Z. Peng, A. Metzger, J. Lin, J. A. Mann, K. Huang, C. Xiang, X. Fan, E. L. G. Samuel, L. B. Alemany, A. A. Martí and J. M. Tour, *ACS Appl. Mater. Interfaces*, 2015, **7**, 7041–7048.

